Circusp34 Promotes Osteosarcoma Proliferation and Invasion by Sponging Mir-16-5p: An in Vivo and in Vitro Analysis

Jingbing Lou
Peking University People's Hospital https://orcid.org/0000-0001-6214-9597
Hongliang Zhang
Peking University People's Hospital
Jiuhui Xu
Peking University People's Hospital
Boyang Wang
Peking University People's Hospital
Tingting Ren
Peking University People's Hospital
Yi Huang
Peking University People's Hospital
Xiaodong Tang (1911210386@bjmu.edu.cn)
Peking University People's Hospital https://orcid.org/0000-0002-0882-5731
Wei Guo
Peking University People's Hospital https://orcid.org/0000-0003-0466-6400

Primary research

Keywords: osteosarcoma, circRNA, miRNA, ceRNA.

Posted Date: May 4th, 2021

DOI: https://doi.org/10.21203/rs.3.rs-428486/v1

Abstract

Background

Osteosarcoma (OS) is a primary and highly malignant mesenchymal tissue tumor. Although it has achieved a significant breakthrough in therapeutic administration, the specific pathological mechanism remains unclear. CircRNAs are a type of covalently circular RNA with a head-to-tail junction site. Several studies have reported that abnormal expression of circRNAs is closely associated with tumorigenesis and progression. CircRNAs promote or inhibit the progression of OS by sponging miRNAs. In this study, we aimed to investigate the endogenous competition between circRNAs and miRNAs in OS.

Methods

CircUSP34 expression was detected by qRT-PCR in KHOS and 143B cells. To confirm the effect of circRNAs and miRNAs, function assays including CCK8, EdU, wound healing, transwell, and western blot were performed in OS cells. FISH and dual-luciferase reporter assays were performed to confirm the sponging mechanism of circUSP34 and miR-16-5p. Additionally, qRT-PCR, immunohistochemistry, HE staining, and western blot were used to confirm the expression of proteins and genes in tumor tissues from mice.

Results

In the present study, we found that circUSP34 promoted OS proliferation, migration, and invasion *in vitro* and *in vivo*. circUSP34 and miR-16-5p were upregulated and downregulated, respectively, in OS cells. OS cells' biological behaviors, such as proliferation, migration, and invasion, were inhibited after circUSP34 knockdown. Western blot results also showed that Vimentin and Ki-67 expression levels were decreased. Similarly, miR-16-5p mimic compromised OS cell proliferation and migration. FISH assay indicated that circUSP34 and miR-16-5p were colocalized in the cytoplasm. The dual-luciferase reporter assay showed that miR-16-5p was sponged by circUSP34. Interestingly, the miR-16-5p mimic partly reversed the inhibitory effect of sh-circUSP34 on the malignancy of OS cells. Finally, animal experiment results about IHC indicated that Vimentin, N-cadherin, and Ki-67 protein expression decreased, but E-cadherin protein expression increased.

Conclusion

Collectively, circUSP34 promoted OS proliferation, migration, and invasion by sponging miR-16-5p. It can serve as a potential therapeutic target and biomarker.

Background

Osteosarcoma (OS) is a primary mesenchymal malignant tumor that commonly occurs in adolescents and young adults [1–6]. Present studies show that a combination of surgery and chemotherapy significantly improves patient prognosis[5]. However, due to its high malignancy and frequent distant metastases, most patients with advanced-stage disease suffer from a terrible prognosis[6]. The initial cause of osteosarcoma remains unclear: its diagnosis and early treatment are thus hindered. Therefore, investigating its pathophysiologic mechanisms and exploring novel therapeutic targets are urgently needed.

Circular RNA(circRNA) is a closed circular RNA formed by back-splicing pre-mRNA and is usually over 200 nucleotides long[7, 8]. Increasing studies have reported that abnormally expressed circRNAs are associated with the clinical characteristics of tumorigenesis, proliferation, metastasis, and invasion[9, 10]. It is often aberrantly expressed in a variety of tumors, such as non-small cell lung cancer, colorectal cancer, and hepatocellular cancer[11–13]. Some circRNAs have oncogenic function, whereas others have anti-tumoral effects[14]. For example, circ_0000285 promotes the proliferation, migration, invasion, but inhibits apoptosis of osteosarcoma by sponging miR-409-3p [15]. Upregulated circ_0028171 in cells competes endogenously with miR-218-5p to promote osteosarcoma progression[16]. Based on the above studies, we speculate that circUSP34 plays an oncogenic role in OS by sponging miR-16-5p.

Materials And Methods

Cell culture

Normal human umbilical vein endothelial cells (HUVEC) and OS cells (KHOS and 143B cell lines) were purchased from the American Type Culture Collection (ATCC, USA). All of them were stored in CELLSAVING solution (New Cell & Molecular Biotech, Suzhou, China) at -80 °C. KHOS cells were cultured in RPMI-1640 (Gibco, Grand Island, NY, USA) and 143B cells were cultured in DMEM (Gibco), and both were supplemented with 10% fetal bovine serum (Gibco), and 1% penicillin and streptomycin (Gibco). Both cell lines were cultured in a humidified incubator with 5% CO^2 at 37 °C.

RNA extraction and quantitative RT-PCR (qRT-PCR)

Total RNA was isolated from OS cells according to the manufacturer's protocol using RNeasy Plus Mini (Qiagen, Germany) and dissolved in 15 μL of RNase free water. The concentration and purification of RNA were assessed using a NanoPhotometer Pearl (IMPLEN, Germany) by measuring the A260/280 absorbance. Complementary DNA (cDNA) was synthesized using PrimeScript RT Master Mix (TaKaRa Biotechnology, Japan). CircUSP34 and miR-16-5p were quantified using iTaq™ Universal SYBR® Green (Bio-Rad, Hercules, CA, USA) with GAPDH and U6 as internal references, respectively. The sequences of primers are listed in Table 1.

Table 1: Sequences of the primers used in the study

		5'→3'
circUSP34	Forward	GCTCCTGTCAGTACACACTCC
	Reverse	GCCATACGATCTAAAAACCACTT
USP34	Forward	CGACTTAGATGCCTTGGCAAGAC
	Reverse	GGAGTCCTGTAAGCCCATCATC
miR-16-5p	Forward	TAGCAGCACGTAAATATTGGCG
	Reverse	TGCGTGTCGTGGAGTC
GAPDH	Forward	GTCTCCTCTGACTTCAACAGCG
	Reverse	ACCACCCTGTTGCTGTAGCCAA
U6	Forward	CTCGCTTCGGCAGCACA
	Reverse	AACGCTTCACGAATTTGCGT

Lentiviruses preparation and oligonucleotide transfection

KHOS and 143B cells were cultured in 6-well plates (8×10^5 cells per well) to 70–80% confluence before transfection. MiR-16-5p mimic and negative control were synthesized by GenePharma (Suzhou, China). Lentivirus, the sh-circUSP34 vector, was constructed targeting the specific head-to-tail junction site purchased from Hanbio Biotechnology Company (Shanghai, China). Lipofectamine 3000 (Invitrogen, Grand Island, NY, USA) and Polybrene (Hanbio Biotechnology Company, Shanghai, China) were applied to facilitate miR-16-5p mimic and sh-circUSP34 complex formation, respectively.

The miR-16-5p mimic sequence is sense:5'-UAGCAGCACGUAAAUAU

UGGCG-3', antisense: 5'-CCAAUAUUUACGUGCUGCUAUU-3', while its negative control is 5'-UUCUCCGAACGUGUCACGUTT-3'.

CCK-8 assay

Three thousand cells per well were cultured in a 96-well plate in triplicate. Subsequently, 10 μL of CCK-8 reagent (Dojindo Crop, Tokyo, Japan) was added to 100 μL of culture medium for 24, 48, 72, and 96 h, according to the manufacturer's instructions. The cells were incubated for 2 h at 37 °C, and the optical density (OD) was measured at 450 nm using a microplate reader (Bio-Rad).

EdU assay

The proliferation ability of cells was evaluated by EdU assay using a BeyoClick EdU Cell Proliferation Kit with Alexa Fluor 555 (Beyotime Biotechnology, Shanghai, China) following the manufacturer's instructions. OS cells were cultured in 12-well plates. Both cell lines were incubated with 10μM EdU

solution for 2h and then fixed using 4% paraformaldehyde. EdU was then examined with Click Additive Solution (Beyotime), and cellular nuclei were stained with Hoechst 33342. EdU cells in five different areas were photographed under a Leica DMi1 microscope (Lecia, Germany). Nuclei were stained by Hoechst 33342 glowing blue under wavelength 346 nm. New synthesized DNA was stained by Azide 555 glowing red under wavelength 565 nm.

Wound-healing assay

KHOS and 143B cells transfected with sh-circUSP34 and sh-NC were seeded in 6-plate plates at 8×10^5 cells per well. When the cell confluence became approximately 80%, a wound line was scratched using a P-200 pipette tip. Next, images were photographed using a microscope (Leica, Germany) at 0 h and after 24 h. The distance between the injury lines was measured and analyzed.

Transwell assay

Briefly, 200 μL serum-free medium containing 5×10^5 cells was added to the upper chamber (Corning, NY, USA) in triplicate. The bottom chamber was filled with 600 μL of medium with 20% FBS. Next, all chambers were incubated at 37 °C for 24 h. The next day, the chambers were fixed with 4% paraformaldehyde and stained with 0.1% crystal violet. Cells in the upper membrane of the chamber were slightly wiped using a swab. Finally, the migrating cells in five different areas were counted under a microscope.

Protein extraction and western blot

The cells were lysed with radioimmunoprecipitation assay lysis buffer (Beyotime, Shanghai, China). Protein concentrations were quantified by a BCA Protein Assay kit (Solarbio, Beijing, China), and equal proteins collected from different types of cell lysates were loaded onto 10% SDS-PAGE gels (Invitrogen) and then transferred onto polyvinylidene difluoride membranes (PVDF). The membranes were blocked with 1× quick blocking buffer diluted from 100× at room temperature and then incubated with primary antibodies anti-vimentin (1:1000, Proteintech, Rosemont, IL, USA), anti-E-cadherin (1:1000, Proteintech), anti-N-cadherin (1:1000, Proteintech), anti-Ki-67 (1:1000, Proteintech), and anti-GAPDH (1:1000, OriGene, Rockville, MD, USA) at 4 °C overnight. Membranes were then washed in TBS-T and incubated with secondary antibodies for 1 h at 37 °C. Proteins were visualized using the Image Lab Software (Bio-rad).

Fluorescence in situ hybridization(FISH) assay

FAM-labeled circUSP34 probes and Cy3-labeled miR-16-5p were designed and synthesized by GenePharma (Shanghai, China). Hybridization was performed overnight at 4 °C with circUSP34 and miR-16-5p probes according to the manufacturer's instructions. Images were acquired on a Nikon Eclipse Ti Scanning Confocal Microscope (Nikon, Japan).

H&E staining and immunohistochemistry

Tissue samples were fixed in 4% paraformaldehyde, embedded in paraffin, and sectioned. The tissue sections were incubated with anti-vimentin (1:5000), anti-N-cadherin (1:1000), anti-E-cadherin (1:1000), and anti-Ki-67(1:8000) primary antibodies at 4 °C overnight and then incubated with an HRP-conjugated secondary antibody. The results were photographed under a microscope.

Animal experimentation

4-week-old female BALB/c nude mice were prepared for the subcutaneous tumor experiments. 143B cells stably transfected with circUSP34 knockdown or negative control were injected subcutaneously (1×10^7, 150 μL). After 21 days, tumors removed from sacrificed mice were subjected to weight comparison, IHC staining, and western blot assay. The animal experiments were approved by the Ethics Committee of Peking University People's Hospital.

Statistical analyses

SPSS software (version 22.0; Chicago, USA) and GraphPad Prism 7 were used for statistical analyses. The data were analyzed by Student's t-test or one-way ANOVA, and the results are presented as the mean ±S.D. No significance is indicated by *ns*. Significant data are indicated by *p < 0.05, **p < 0.01, and ***p < 0.001.

Results

The character and expression level of circUSP34 in OS cells

To better understand the features of circUSP34, we depicted its location on the chromosome. Data from circBank (http://www.circbank.cn/index.html) and UCSC (http://genome.ucsc.edu/) showed that circUSP34, which is derived from chr.2p14, exhibited a circular structure via post-transcriptional head-to-tail splicing (Fig.1a). It has been reported that circRNA, including circUSP34 which is relatively stable, was resistant to RNase R digestion[17]. To verify this, RNase R treatment was initially performed. Subsequently, we designed divergent and convergent primers to verify the differentiation of circUSP34 with and without RNase R treatment using qRT-PCR. The results showed that circUSP34 was not digested, but USP34 mRNA was (Fig. 1b). Agarose gel electrophoresis was also performed to examine the product of qRT-PCR and confirmed that circUSP34 was resistant to RNase R digestion (Fig. 1c), as opposed to USP34 mRNA. qRT-PCR revealed circUSP34 had upregulated expression in both 143B and KHOS cells (Fig. 1d). Therefore, we verified the circular structure and stability of circUSP34. Meanwhile it was up-regulated in OS cells

CircUSP34 knockdown inhibits OS cell malignancy, especially proliferation and migration

The above observations prompted us to further investigate the potential role of circUSP34 in OS cells. Loss-of-function assays were also performed. Then, 143B and KHOS cells were transfected with sh-circUSP34 to knock down circUSP34 expression, which was confirmed by qRT-PCR. The results showed

that its expression level significantly decreased in both cell lines (Fig. 2a). To determine the role of sh-circUSP34 in proliferation viability *in vitro*, both CCK8 and EdU assays were performed. All results revealed that interfering circUSP34 compromised the proliferation ability of 143B and KHOS cells (Fig. 2b and c). Moreover, the colony formation assay also indicated that silencing circUSP34 suppressed the proliferation potential of OS cells, which was consistent with the above results (Fig. 2d). Overall, these results suggested that silencing circUSP34 inhibited the proliferation of OS cells.

Transwell migration with invasion and wound healing assays were carried out to further explore the effect of sh-circUSP34 on OS cell migration or aggression. A wound-healing assay showed that migration capacity was inhibited in 143B and KHOS cell lines transfected with sh-circUSP34 compared to the NC group (Fig. 2e). Transwell migration and invasion assays demonstrated that migration and invasion were inhibited (Fig. 2f). Therefore, these results demonstrate that circUSP34 knockdown suppressed both migration and invasion.

Furthermore, western blot results indicated that Vimentin expression decreased after circUSP34 knockdown. Meanwhile, Ki-67 protein expression levels were also downregulated (Fig. 2g). Taken together, our data indicate that silencing circUSP34 can inhibit the progression of OS *in vitro*.

CircUSP34 sponges miR-16-5p to regulate OS cell malignancy

Given the interaction of both, first, the target site was predicted by Starbase (http://starbase.sysu.edu.cn/starbase2) as shown in Fig. 3a. Second, we performed a FISH assay to colocalize circUSP34 (green) and miR-16-5p (red) in OS cells: both co-localized in the cytoplasm (Fig. 3b). Third, miR-16-5p relative expression level was detected by qRT-PCR in OS cells transfected with sh-circUSP34, which obviously increased (Fig. 3c). Finally, a dual-luciferase reporter assay was performed on the OS cells. The results showed that the luciferase activity of the circUSP34-WT group with miR-16-5p mimic group obviously decreased compared with miR-16-5p mimic NC group (Fig. 3d). As evidenced by the above results, we hypothesized that miR-16-5p was sponged by circUSP34 to promote OS.

MiR-16-5p inhibits malignancy of OS *in vitro*

We next explored miR-16-5p expression in KHOS and 143B cells. qRT-PCR data showed that miR-16-5p expression was significantly downregulated in OS cells compared with normal HUVECs (Fig. 4a). To confirm the possible anti-tumor effect of miR-16-5p, we designed a miRNA mimic to elevate miR-16-5p expression levels. Subsequently, the inhibitory effect of miR-16-5p mimic on proliferation, migration, and invasion was studied using several assays. CCK-8 assay results showed that miR-16-5p suppressed the proliferation of KHOS and 143B cells (Fig. 4b). To perform double verification, an EdU assay was adopted, which exhibited increased inhibition in OS cells *in vitro* (Fig. 4c). Similarly, the proliferation ability was evaluated *in vitro* using a colony-forming assay (Fig. 4f). The miR-16-5p mimic comprised the migration ability of KHOS and 143B cells, as confirmed by the wound healing assay (Fig. 4d). Transwell assay results revealed that the migration and invasion abilities were inhibited by upregulated miR-16-5p

(Fig. 4e). Our results show evidence that miR-16-5p plays a suppressive role in malignancy progression *in vitro*.

MiR-16-5p inhibitor reversed the anti-tumor function of sh-circUSP34

To clarify the specific relationship between miR-16-5p and circUSP34, OS cells treated with sh-circUSP34 were transfected with miR-16-5p inhibitor. The efficacy of transfection was quantified using qRT-PCR. The results showed that miR-16-5p expression level decreased, but that of circUSP34 increased (Fig. 5a). EdU and CCK8 results indicated that the miR-16-5p inhibitor rescued the inhibitory effect of sh-circUSP34 on OS cell viability (Fig. 5b and c). The results showed that miR-16-5p activates the promotion effect of circUSP34 on proliferation. Wound healing assay results indicated that the inhibitory function of sh-circUSP34 was rescued by the miR-16-5p inhibitor (Fig. 5d). Collectively, these results showed that circUSP34 served as a sponge for miR-16-5p to regulate OS malignancy.

Silencing circUSP34 inhibits proliferation and metastasis of OS cells *in vivo*

To confirm the oncogene function of circUSP34 *in vivo*, we constructed six BALB/c nude mice models. Every week, the tumor volumes in both groups were measured, showing that tumor weight and volume in the sh-circUSP34 group was inhibited significantly comparing with the sh-NC group (Fig. 6a–d). We performed qRT-PCR to detect miR-16-5p expression levels in tumor tissues. The results showed an increased expression level in the sh-circUSP34 group (Fig. 6e). Subsequently, the H&E staining results indicated that it was consistent with the pathological characteristics of OS (Fig. 6f). Additionally, immunocytochemistry results showed that Vimentin, N-cadherin, and Ki-67 protein expression decreased, but E-cadherin protein expression increased (Fig. 6g). Simultaneously, western blot results also indicated that OS malignancy was markedly compromised. Vimentin, N-cadherin, and Ki-67 expression levels were elevated significantly; however, E-cadherin expression levels increased (Fig. 6h). These results suggest that circUSP34 may act as an oncogene to promote OS development by sponging miR-16-5p.

Discussion

Although osteosarcoma is a relatively rare malignant tumor derived from mesenchymal tissue, its high-grade malignancy, especially distant metastasis, cannot be neglected. The combination of surgery and chemotherapy markedly improves patients' prognosis [18]. However, local invasion, metastasis, and drug resistance are still to be improved [18, 19]. Exploring an effective therapeutic target is an urgent and critical issue. An increasing number of studies has shown that circRNAs are aberrantly expressed in a variety of tumors involving OS [20, 21]. For instance, high expression of circRNA can promote the invasion ability of gastrointestinal cancer, lung cancer, and liver cancer [22-24]. Thus, we predicted circUSP34 by Starbase as an upstream "sponge" of miR-16-5p, which was reported to inhibit OS[25]. In the present study, the expression level of circUSP34 was confirmed by qRT-PCR, which showed high expression compared to the normal control. Epithelial-mesenchymal transition (EMT) is considered to play a significant role in malignancy progression, such as metastasis, in OS. To confirm the effect of circUSP34 on EMT-related proteins of OS, vimentin, E-cadherin, N-cadherin protein expression was

quantified by western blot. Loss-of-function assays verifying the oncogene circUSP34 in KHOS and 143B cells showed that knocking out circUSP34 compromised the malignant biological behavior of OS cells *in vitro*. Low expression of circUSP34 inhibits tumor growth *in vivo* by establishing subcutaneous tumors in mice.

It is widely accepted that miRNA function is modulated by circRNA sponging in various pathological and pathophysiological activities[26, 27]. Circ_NOTCH3 competes with miR-205-5p to promote the progression of basal-like breast carcinoma [28]. Circular RNA MYLK, a competing endogenous RNA, promotes bladder cancer progression[29]. Moreover, miR-622 is sponged by circ_0119872 to promote uveal melanoma development[30]. It is worth noting that not every circRNA can sponge miRNAs to modulate their biological functions, as their activity has several requirements, such as a consistent subcellular location. Although miR-16-5p has been previously reported to impede tumor growth[25], in our study, we confirmed its inhibitory function. Low expression level was quantified by performing qRT-PCR, but it significantly increased after circUSP34 knockdown. This result further supported the hypothesis of interaction between circUSP34 and miR-16-5p. Similarly, gain-of-function assays results showed that overexpression of miR-16-5p impeded OS development. Therefore, it is increasingly possible credible for circUSP34 to sponge miR-16-5p. To better understand circUSP34 as a sponge of miR-16-5p, a rescue experiment was performed. Most importantly, Zhang et al reported that Smad3 acts as a target of miR-16-5p in chordoma cells[31]. Therefore, we speculate that miR-16-5p inhibits OS malignancy by targeting Smad3. Further studies are needed to explore the underlying mechanism.

In conclusion, our results revealed that circUSP34 promotes OS proliferation, migration, and invasion rather than apoptosis by sponging miR-16-5p. However, it was negatively correlated with tumor size *in vivo*. Moreover, circUSP34 could serve as a potential therapeutic target and a predictable biomarker.

Conclusion

In summary, our findings revealed that highly regulated circUSP34 plays a role in oncogenes and underlying biomarkers in OS. Furthermore, circUSP34 may be a potential therapeutic target for OS. We first demonstrated that circUSP34 promotes OS proliferation, migration, and invasion by sponging miR-16-5p. However, our study needed further exploration of the mechanism of circUSP34 and its clinicopathological correlation with OS patients.

Abbreviations

CircRNA, circular RNA; miRNA, microRNA; BCA, bicinchoninic acid; EMT, epithelial-mesenchymal transition; FISH, Fluorescence in situ hybridization; OD, optical density. Complementary DNA, cDNA.

Declarations

Ethics approval and consent to participate

This study was conducted in accordance with the recommendations of the Guide for Chinese Ethics Review Committees. The protocol was approved by the Ethics Committee of Peking University People's Hospital.

The animal experiments were approved by the Ethics Committee of Peking University People's Hospital.

Consent for publication

Not applicable.

Availability of data and materials

Corresponding authors provided data and materials in a reasonable way.

Competing interests

The authors declare that they have no conflict of interest.

Funding

This work was supported by the National Natural Science Foundation of China (No. 81972509).

Authors' contributions

JL, XT, and WG designed and performed the experiment. JL and HZ performed experiments, wrote the manuscript, and analysed data. JX, BW, TR, and YH collected and interpreted data. All authors have read and approved the final manuscript.

Acknowledgements

Not applicable.

References

1. Chen Chenglong M, Xingjia C, Caitong J, Yurui Z, Yi R, Tingting, et al. miR-135a Reduces Osteosarcoma Pulmonary Metastasis by Targeting Both BMI1 and KLF4. Front Oncol. 2021;11:620295.
2. Huang Q, Liang X, Ren T, Huang Y, Zhang H, Yu Y, et al. The role of tumor-associated macrophages in osteosarcoma progression - therapeutic implications. Cell Oncol (Dordr). 2021.
3. Zhang H, Wang J, Ren T, Huang Y, Yu Y, Chen C, et al. LncRNA CASC15 is Upregulated in Osteosarcoma Plasma Exosomes and CASC15 Knockdown Inhibits Osteosarcoma Progression by Regulating miR-338-3p/RAB14 Axis. Onco Targets Ther. 2020;13:12055–66.
4. Niu J, Yan T, Guo W, Wang W, Zhao Z, Ren T, et al. Identification of Potential Therapeutic Targets and Immune Cell Infiltration Characteristics in Osteosarcoma Using Bioinformatics Strategy. Front Oncol.

2020;10:1628.

5. Lilienthal I, Herold N. Targeting Molecular Mechanisms Underlying Treatment Efficacy and Resistance in Osteosarcoma: A Review of Current and Future Strategies. Int J Mol Sci. 2020;21(18):6885.
6. Duffaud F. Role of TKI for Metastatic Osteogenic Sarcoma. Curr Treat Options Oncol. 2020;21(8):65.
7. Ragan C, Goodall GJ, Shirokikh NE, Preiss T. Insights into the biogenesis and potential functions of exonic circular RNA. Sci Rep. 2019;9(1):2048.
8. Hou LD, Zhang J. Circular RNAs: An emerging type of RNA in cancer. Int J Immunopathol Pharmacol. 2017;30(1):1–6.
9. Jafari Ghods F. Circular RNA in Saliva. Adv Exp Med Biol. 2018;1087:131–9.
10. Wang S, Zhang X, Li Z, Wang W, Li B, Huang X, et al. Circular RNA profile identifies circOSBPL10 as an oncogenic factor and prognostic marker in gastric cancer. Oncogene. 2019;38(44):6985–7001.
11. Wei S, Zheng Y, Jiang Y, Li X, Geng J, Shen Y, et al. The circRNA circPTPRA suppresses epithelial-mesenchymal transitioning and metastasis of NSCLC cells by sponging miR-96-5p. EBioMedicine. 2019;44:182–93.
12. Long F, Lin Z, Li L, Ma M, Lu Z, Jing L, et al. Comprehensive landscape and future perspectives of circular RNAs in colorectal cancer. Mol Cancer. 2021;20(1):26.
13. Liu G, Sun J, Yang ZF, Zhou C, Zhou PY, Guan RY, et al. Cancer-associated fibroblast-derived CXCL11 modulates hepatocellular carcinoma cell migration and tumor metastasis through the circUBAP2/miR-4756/IFIT1/3 axis. Cell Death Dis. 2021;12(3):260.
14. Qiu L, Xu H, Ji M, Shang D, Lu Z, Wu Y, et al. Circular RNAs in hepatocellular carcinoma: Biomarkers, functions and mechanisms. Life Sci. 2019;231:116660.
15. Long Z, Gong F, Li Y, Fan Z, Li J, et al. Circ_0000285 regulates proliferation, migration, invasion and apoptosis of osteosarcoma by miR-409-3p/IGFBP3 axis. Cancer Cell Int. 2020;20:481.
16. Pan F, Zhang J, Tang B, Jing L, Qiu B, Zha Z. The novel circ_0028171/miR-218-5p/IKBKB axis promotes osteosarcoma cancer progression. Cancer Cell Int. 2020;20:484.
17. Ma S, Kong S, Wang F, Ju S. CircRNAs: biogenesis, functions, and role in drug-resistant Tumours. Mol Cancer. 2020;19(1):119.
18. Fernandes I, Melo-Alvim C, Lopes-Brás R, Esperança-Martins M, Costa L. Osteosarcoma Pathogenesis Leads the Way to New Target Treatments. Int J Mol Sci. 2021;22(2):813.
19. Marchandet L, Lallier M, Charrier C, Baud'huin M, Ory B, Lamoureux F. Mechanisms of Resistance to Conventional Therapies for Osteosarcoma. Cancers (Basel). 2021;13(4):683.
20. Chen J, Yang J, Fei X, Wang X, Wang K. CircRNA ciRS-7: a Novel Oncogene in Multiple Cancers. Int J Biol Sci. 2021;17(1):379–89.
21. Li Z, Li X, Xu D, Chen X, Li S, Zhang L, et al. An update on the roles of circular RNAs in osteosarcoma. Cell Prolif. 2021;54(1):e12936.

22. Zong L, Sun Q, Zhang H, Chen Z, Deng Y, Li D. Increased expression of circRNA_102231 in lung cancer and its clinical significance. Biomed Pharmacother. 2018;102:639–44.
23. Lin Q, Ling YB, Chen JW, Zhou CR, Chen J, Li X, et al. Circular RNA circCDK13 suppresses cell proliferation, migration and invasion by modulating the JAK/STAT and PI3K/AKT pathways in liver cancer. Int J Oncol. 2018;53(1):246–56.
24. Li P, Chen S, Chen H, Mo X, Li T, Shao Y, et al. Using circular RNA as a novel type of biomarker in the screening of gastric cancer. Clin Chim Acta. 2015;444:132–6.
25. Gu Z, Li Z, Xu R, Zhu X, Hu R, Xue Y, et al. miR-16-5p Suppresses Progression and Invasion of Osteosarcoma via Targeting at Smad3. Front Pharmacol. 2020;11:1324.
26. Nisar S, Bhat AA, Singh M, Karedath T, Rizwan A, Hashem S. Insights Into the Role of CircRNAs: Biogenesis, Characterization, Functional, and Clinical Impact in Human Malignancies. Front Cell Dev Biol. 2021;9:617281.
27. Wang X, Li H, Lu Y, Cheng L. Circular RNAs in Human Cancer. Front Oncol. 2020;10:577118.
28. Guan B, Li Q, Zhang HZ, Yang HS. circ_NOTCH3 Functions as a Protooncogene Competing With miR-205-5p, Modulating KLF12 Expression and Promoting the Development and Progression of Basal-Like Breast Carcinoma. Front Oncol. 2020;10:602694.
29. Zhong Z, Huang M, Lv M, He Y, Duan C, Zhang L, et al. Circular RNA MYLK as a competing endogenous RNA promotes bladder cancer progression through modulating VEGFA/VEGFR2 signaling pathway. Cancer Lett. 2017;403:305–17.
30. Liu S, Chen L, Chen H, Xu K, Peng X, Zhang M. Circ_0119872 promotes uveal melanoma development by regulating the miR-622/G3BP1 axis and downstream signalling pathways. J Exp Clin Cancer Res. 2021;40(1):66.
31. Zhang H, Yang K, Ren T, Huang Y, Tang X, Guo W. miR-16-5p inhibits chordoma cell proliferation, invasion and metastasis by targeting Smad3. Cell Death Dis. 2018;9(6):680.

Figures

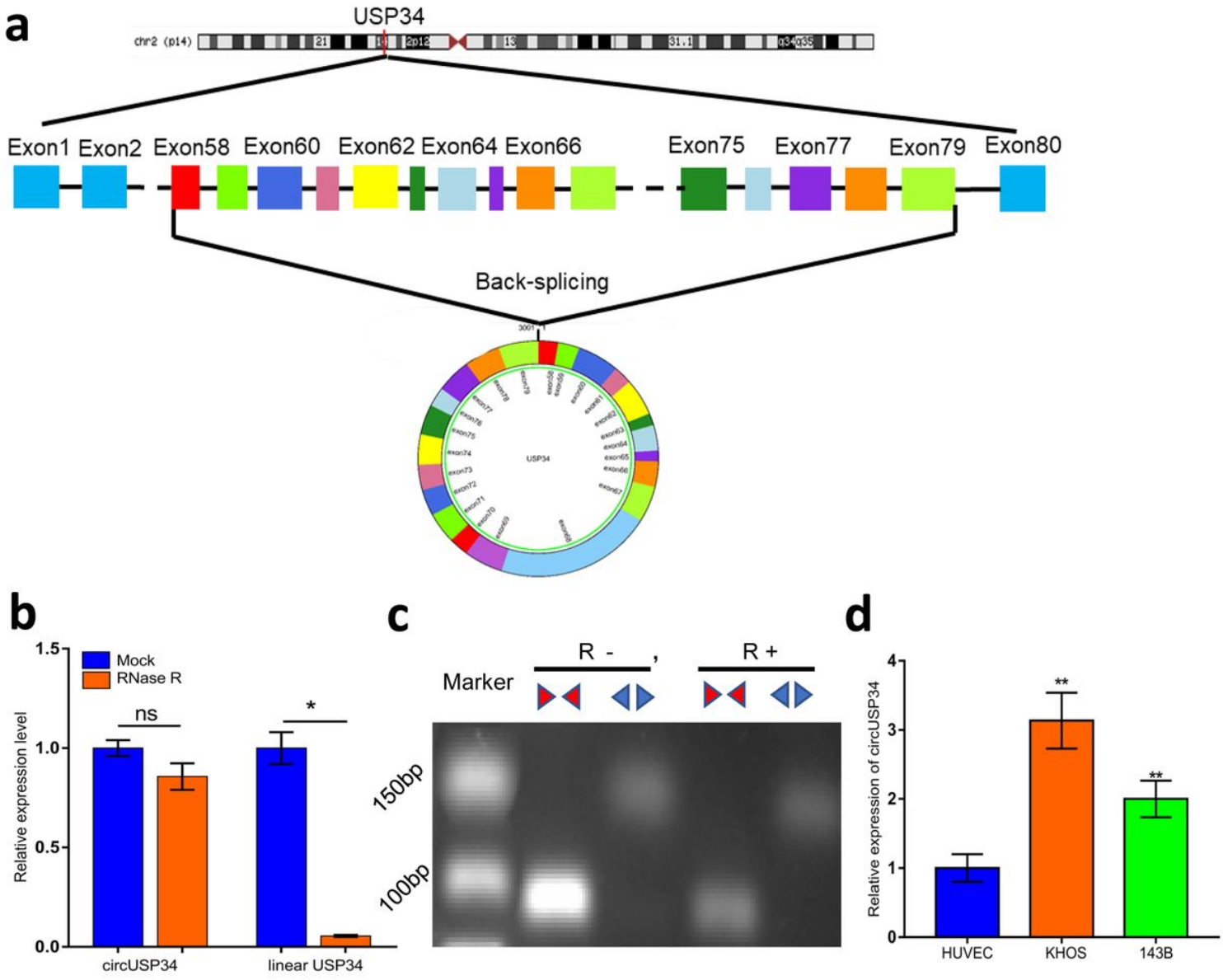

Figure 1

The character and expression level of circUSP34 in OS cells. a. We depicted the head-to-tail back-splicing form by UCSC and circBank. b and c. The stability and existence of circUSP34 in 143B cell were detected by qRT-PCR and nucleic acid electrophoresis. d. CircUSP34 expression level in OS cells was confirmed by qRT-PCR. Data were showed as mean ± SD. ns indicated no significance, *P < 0.05, **P < 0.01.

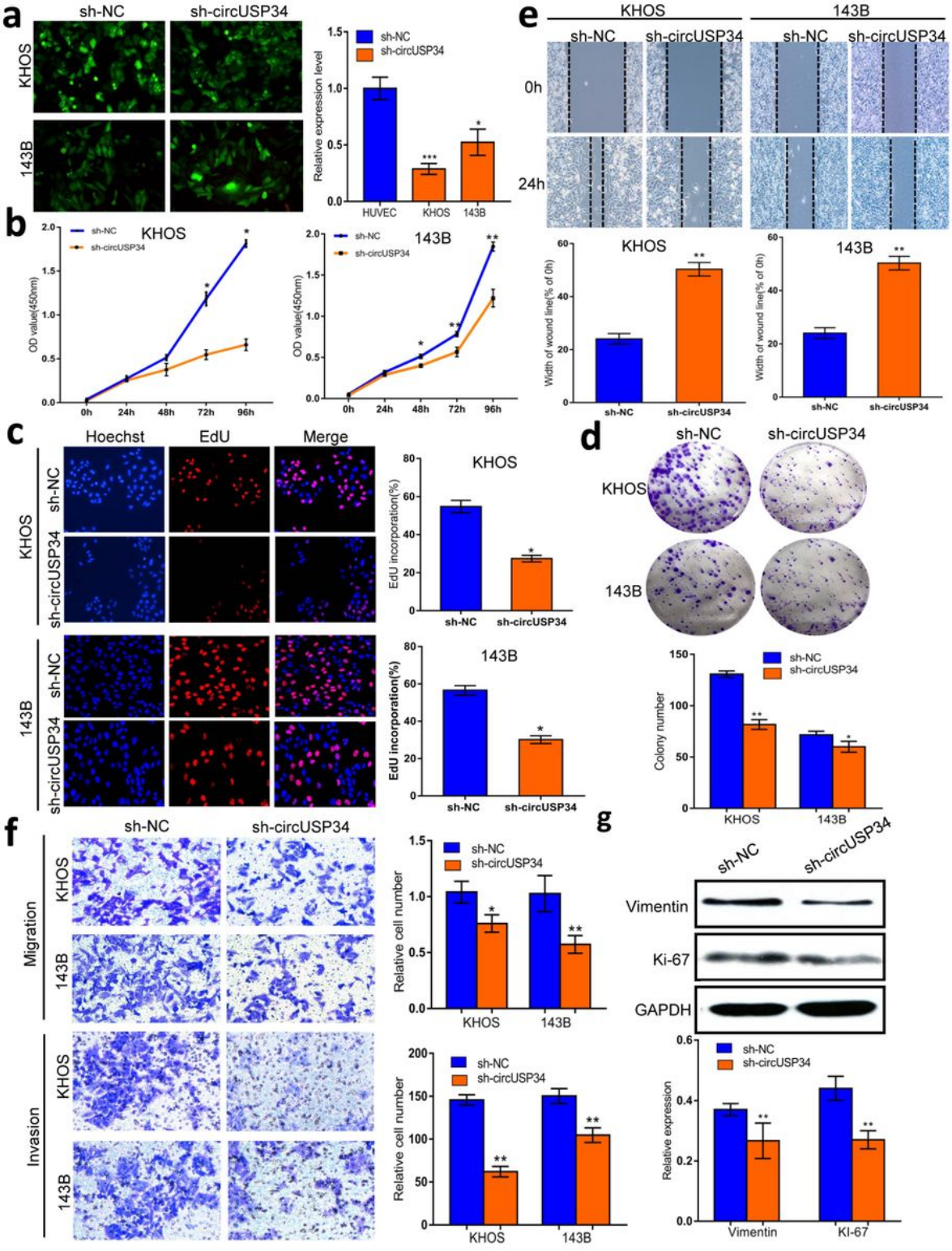

Figure 2

CircUSP34 knockdown inhibits OS cell malignancy, especially proliferation and migration. a. Scenes of both KHOS and 143B cells transfected by sh-circUSP34 and sh-NC vector were photographed. And knock-out efficacy was quantified by qRT-PCR. b,c and d. EdU,CCK8 and colony formation assays results showed that proliferation was inhibited in KHOS and 143B cells transfected by sh-circUSP34 or sh-NC. e and f. OS cells' migration and invasion ability were evaluated by wound healing as well as transwell

assays. g. Vimentin and Ki-67 protein expression was assessed by western blot. Data were showed as mean ± SD. *P < 0.05, **P < 0.01, ***P < 0.001.

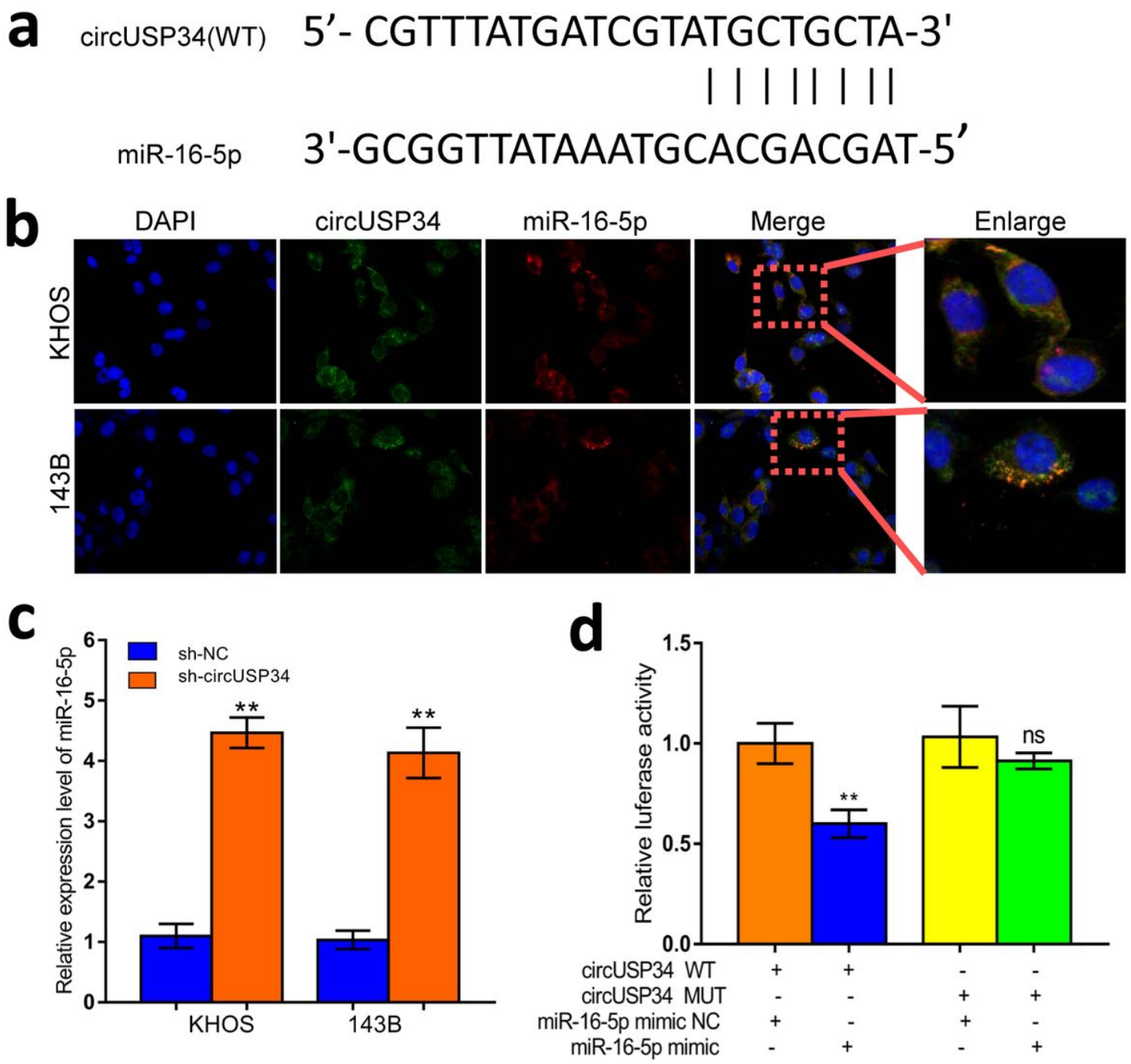

Figure 3

CircUSP34 sponges miR-16-5p to regulate OS cell malignancy. a. The possible target site between circUSP34 and miR-16-5p was predicted by Starbase. b. The cellular location of circUSP34 (green) and miR-16-5p (red) in cells was observed by performing FISH (magnification, 400×, scale bar, 100 μm). c. miR-16-5p expression level was confirmed by qRT-PCR after transfecting sh-circUSP34. d. The relative luciferase activities were detected in 293T cells after co-transfection with circUSP34-WT or circUSP34-

MUT and mimics, or NC, respectively. Data were showed as mean ± SD. *P < 0.05, **P < 0.01, ***P < 0.001.

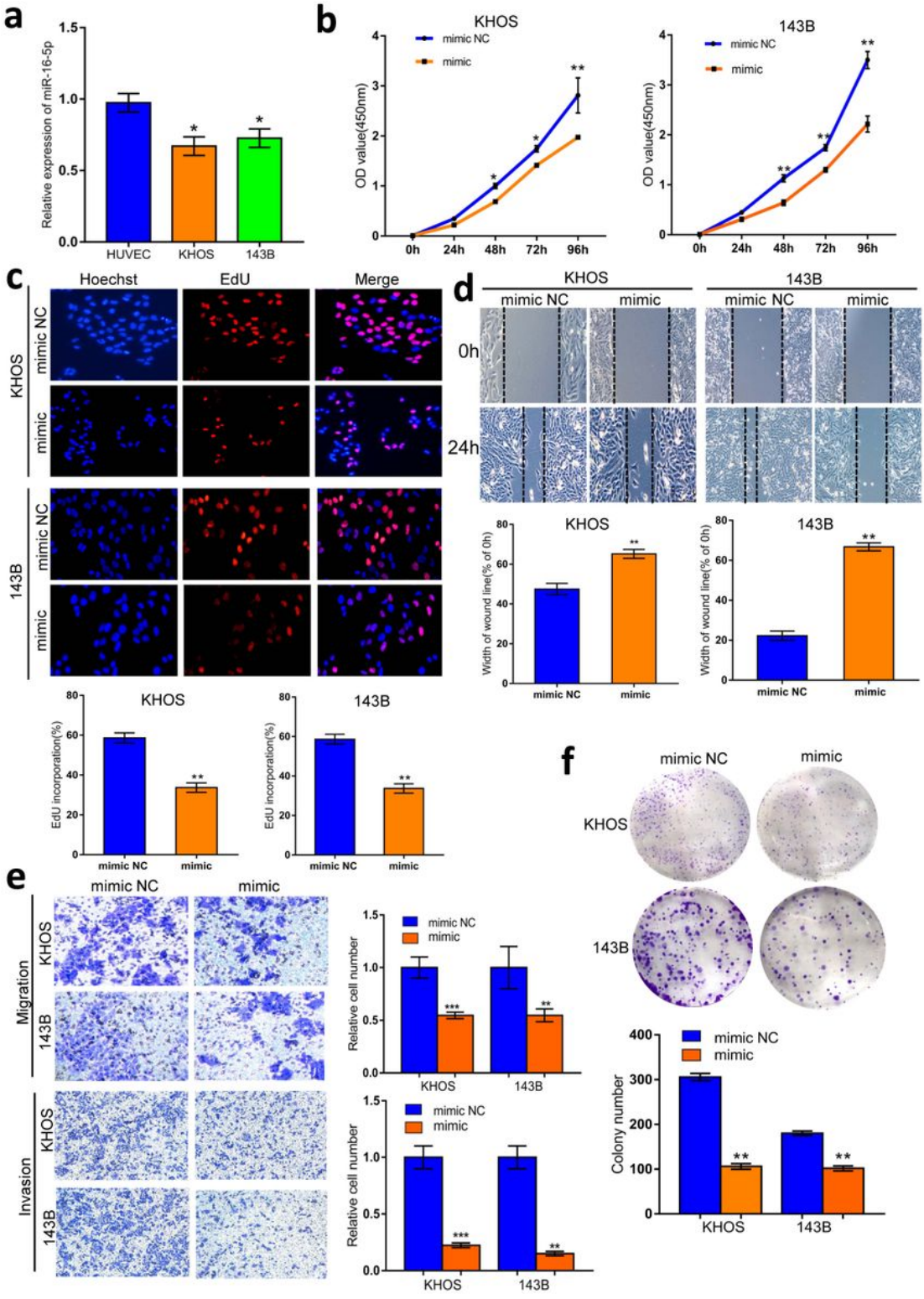

Figure 4

miR-16-5p inhibits malignancy of OS in vitro. a. The expression level of miR-16-5p was confirmed by qRT-PCR. b and c. CCK8 and EdU assays showed that proliferation viability was inhibited by mimic in both OS cells. d and e. Wound healing and transwell assays indicated migration and invasion capacity was

suppressed in vitro. f. Colony formation results showed that proliferation ability was suppressed. Data were showed as mean ± SD. *P < 0.05, **P < 0.01, ***P < 0.001.

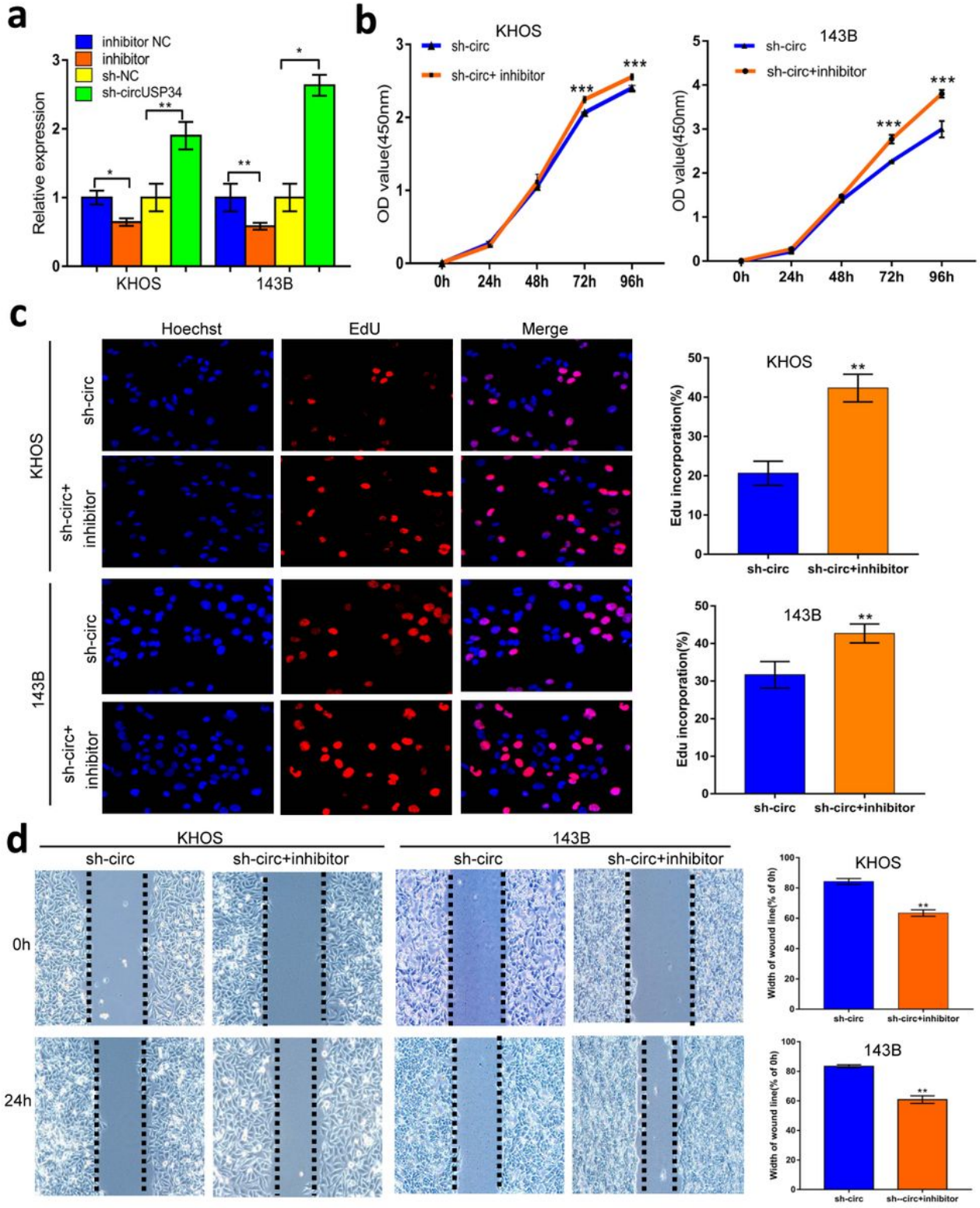

Figure 5

miR-16-5p inhibitor reversed the anti-tumor function of sh-circUSP34. a. The expression level miR-16-5p and circUSP34 with inhibitor and sh-circUSP34 was confirmed by qRT-PCR respectively. b and c. CCK8 and EdU assays showed that the inhibitory function of sh-circUSP34 was rescued by miR-16-5p inhibitor.

d. The effect of miR-16-5p inhibitor on migration in OS cells transfected by sh-circUSP34 was verified by wound healing assay. Data were showed as mean ± SD. *P < 0.05, **P < 0.01, ***P < 0.001.

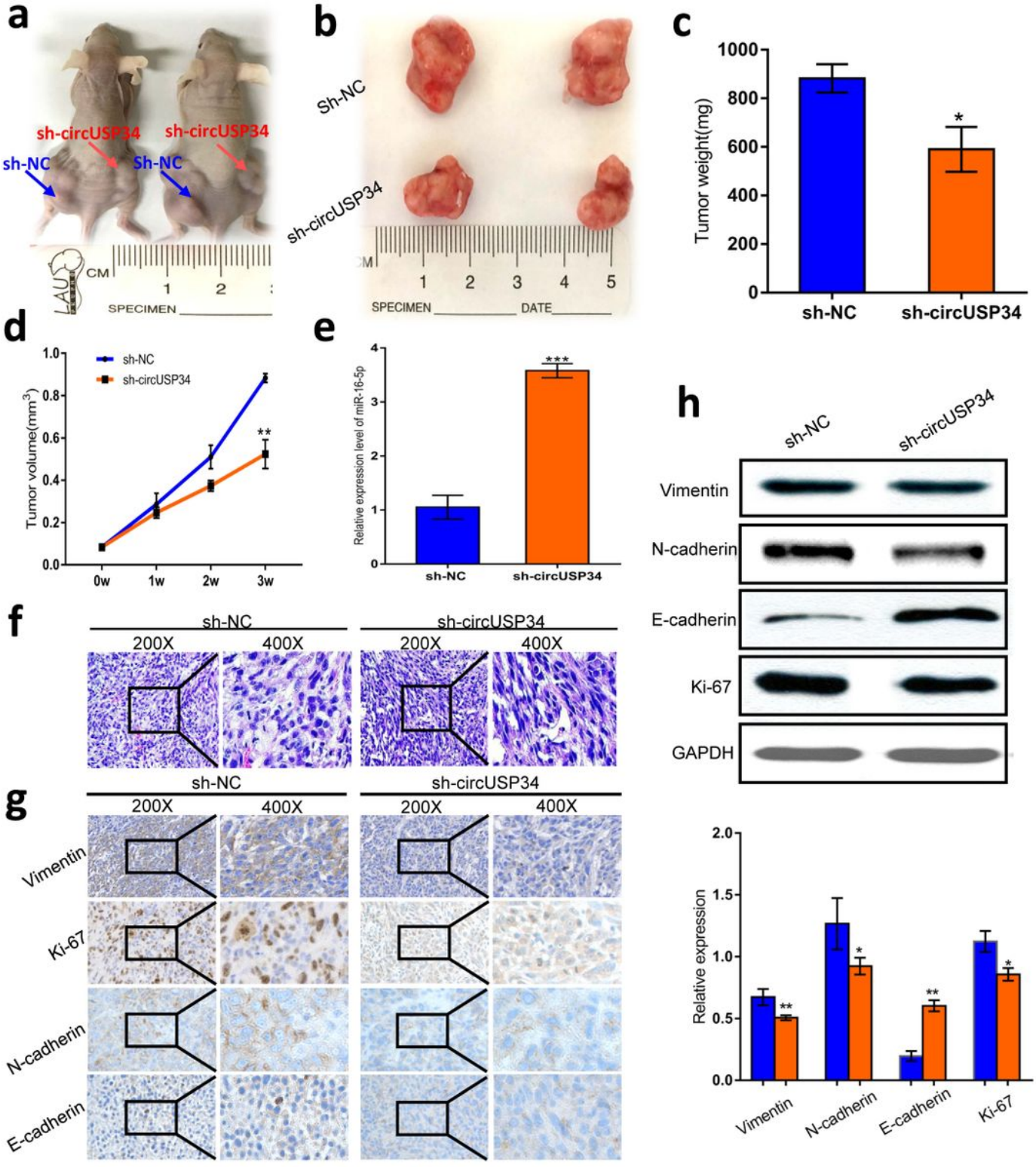

Figure 6

Sliencing circUSP34 inhibits proliferation and metastasis of OS cells in vivo. a and b. Subcutaneous tumors of circUSP34-knockout and NC. c. Tumor weight was measured in sh-circUSP34 and sh-NC group which was analyzed. d. Tumor volume was measured every week. e. Relative expression level of miR-16-

5p was quantified in tumor tissue by qRT-PCR. f. Representative images of HE staining were exhibited from sh-circUSP34 group and sh-NC group. g. The expression of Vimentin, Ki-67, N-cadherin, and E-cadherin were evaluated by performing IHC. h. Western blot assay showed protein expression level of Vimentin, Ki-67, N-cadherin and E-cadherin from tumor tissue. Data were showed as mean ± SD. *P < 0.05, **P < 0.01, ***P < 0.001.